Molecular Crystals and Liquid Crystals

Publication details, including instructions for authors and subscription information:
http://www.tandfonline.com/loi/gmcl20

Conformational Kinetics of Aliphatic Tails

Alberta Ferrarini [a], Giorgio Moro [a] & Pier Luigi Nordio [a]

[a] Department of Physical Chemistry, University of Padua, Padova, 35131, Italy

Version of record first published: 18 Oct 2010

To cite this article: Alberta Ferrarini, Giorgio Moro & Pier Luigi Nordio (2003): Conformational Kinetics of Aliphatic Tails, Molecular Crystals and Liquid Crystals, 394:1, 59-86

To link to this article: http://dx.doi.org/10.1080/15421400390226146

Mol. Cryst. Liq. Cryst., Vol. 394, pp. lix–lxxxvi, 2003

ISSN 1542-1406 print/1563-5287 online
DOI: 10.1080/15421400390226146

Taylor & Francis
Taylor & Francis Group

CONFORMATIONAL KINETICS OF ALIPHATIC TAILS

Alberta Ferrarini, Giorgio Moro and Pier Luigi Nordio
Department of Physical Chemistry, University of Padua, 35131 Padova, Italy

The master equation describing the random walk between sites identified with the stable conformers of a chain molecule, represents the extension to the time domain of the Rotational Isomeric State model. The asymptotic analysis of the multidimensional diffusion equation in the continuous torsional variables subjected to the configurational potential, provides a rigorous justification for the discrete models, and it supplies, without resorting to phenomenological parameters, molecular definitions of the kinetic rates for the conformational transitions occurring at each segment of the chain. The coupling between the torsional variables is fully taken into account, giving rise to cooperative effects.

A complete calculation of the specific correlation functions which describe the time evolution of the angular functions probed by N.M.R. and dielectric relaxation measurements, has been performed for alkyl chains attached to a massive core. The resulting behaviour has been compared with the decay of trans and gauche populations of specific bonds, expressed in terms of suitable correlation functions whose time integrals lead quite naturally to the definition of effective kinetic constants for the conformational transitions.

1. INTRODUCTION

The interpretation of the dynamical processes occurring in molecular systems with many internal degrees of freedom is a challenge for any theorist acquainted with the mathematical tools of statistical mechanics. In principle, the problem could be addressed by a variety of methods, notably by employing Molecular Dynamics (MD), Brownian Dynamics (BD) or stochastic equations, such as Fokker–Planck (FP) or diffusion-type equations. In practice, severe difficulties may arise in the presence of relatively

Received 8 July 1987; accepted 16 October 1987.

This work has been supported by the Italian Ministry of Public Education, and in part by the National Research Council through its Centro Studi sugli Stati Molecolari, Radicalici ed Eccitati. The authors thankfully acknowledge Dr. F. Coletta and Professor U. Segre for enlightening discussions.

high hindering potentials, because of the intrinsically long time scale of the conformational changes. This fact poses severe limitations to both MD and BD methods, requiring enormously long computational times, or to the numerical solution of stochastic equations, because of the impossibly large function set required for the matrix representation of the time evolution operator.

It is quite obvious that the solution of the problem of flexible chains can be addressed only by a discretization of the dynamical equations, essentially resorting to the Rotational Isomeric State (RIS) approximation in the form widely discussed by Flory [1]. In fact, a large amount of work has been performed in this direction, even if a self-consistent, fully rigorous approach still appears to be lacking. It might be useful to summarize the main stages in the progress of understanding the nature of the complex motions occurring in aliphatic chains, by recalling some of the most significant contributions which have appeared in the literature of the last two decades. Wallach [2] was the first to face the problem of multiple internal rotations, that however were assumed to be completely factorized. Levine *et al.* [3] included the anisotropy of the overall diffusion but adopted only one phenomenological rate constant to describe the internal motions. The energetics of the trans-gauche isomerism was introduced in the Wallach model by London and Avitable [4]. Wittebort and Szabo [5] relaxed the assumption of independent internal motions, but still used phenomenological transition rates. Edholm and Blomberg [6] pointed out the applicability to conformational problems of the general theory for kinetic rates derived in the pioneering work of Kramers [7]. Helfand and Skolnick [8, 9] used the mathematical analysis outlined by Langer [10] for the solution of multivariate FP equations, to interpret cooperative effects that make the swinging of long tails against frictional forces feasible. In a different area, great interest attaches to the papers by Levy, Karplus and coworkers, [11, 12], which employed BD methods for studying the liquid alkanes. As already mentioned, this method suffers up to now from the intrinsic limitation that only few conformational events occur in the time scale scanned by the computations.

We feel that a conclusive step to be performed is the rigorous derivation of the correlation functions or spectral densities for the relevant dynamical variables, able to link the master equations used in connection with the RIS approximation to the multivariate FP or diffusion equations, and to avoid *ad hoc* assumptions or loosely defined phenomenological parameters. We will show here that this can be done in the overdamped frictional regime, a condition normally satisfied for most liquids. We shall also see that no free parameter is left if hydrodynamic models [13] are employed to evaluate the friction exerted by the viscous medium upon the flexible molecules, in dependence of its conformational geometry.

In previous papers [14, 15] we have shown how a continuous diffusion equation can be reduced to a master equation for a random walk among discrete sites, by a projection of the diffusion operator onto the subspace of 'site functions' localized at the potential minima. Although the derivation was obtained for single variable problems, we shall show that multidimensional cases can be effectively reduced to one dimension if the reaction pathway connecting two potential minima can be identified. When this is not directly attainable from the symmetry properties of the problem [16], reasonably approximate solutions can be generated by normal mode analysis following quadratic expansion of the intramolecular potential around the saddle points, according to Langer's procedure [10]. As previously mentioned, this method overcomes the assumption of independent variables, and it supplies solutions for the full multidimensional equations.

The theoretical methods developed here, apart from their direct application to conformational kinetics, are expected to supply a rigorous foundation for the general problem of the chemical kinetics. The localized functions may be used to define 'species specification functions' [17], and the matrix elements between these functions can be related to specific kinetic rates. The problem of the chemical kinetics, following the fundamental work of Kramers [7], has been revisited by many authors with various approaches based on correlation function [18–20] or escape time [21–23] concepts. The relationships with standard transition state theory (TST) have also been investigated. A critical review of the current state of knowledge of dynamical processes among metastable states can be found in a recent article by Hänggi [24].

2. DISCRETIZATION OF THE DIFFUSION EQUATION

The mathematical method suitable for the conversion of the diffusion equation in a continuous variable into a random walk between discrete sites, has been already described [14, 15] for one dimensional problems. The procedure will however be summarized here. The diffusion equation can be written as:

$$\begin{aligned}(\partial/\partial t)P(x,t) &= (\partial/\partial x)D(x)P(x)(\partial/\partial x)P(x)^{-1}P(x,t)\\ &= -\hat{\boldsymbol{R}}P(x,t),\end{aligned} \tag{1}$$

where $D(x)$ is the diffusion coefficient with a dependence upon the variable x retained for sake of generality, and $P(x)$ is the equilibrium distribution function expressed in terms of an internal potential $V(x)$ by the Boltzmann relation:

$$P(x) = Z^{-1}\exp\{-V(x)/kT\}, \tag{2}$$

The potential $V(x)$ is assumed to have M minima at the coordinates $x_m, m = 1, 2, \ldots, M$. In correspondence of each minimum, a localized function $g_m(x)P(x)$ is defined in the interval $x_{m-1} \leq x \leq x_{m+1}$ by the expression

$$g_m(x) = \int_{x_{m\pm1}}^{x} dy\{D(y)P(y)\}^{-1} \Big/ \int_{x_{m\pm1}}^{x_m} dy\{D(y)P(y)\}^{-1}. \tag{3}$$

The positive or negative sign in the integration limit refers to $x < x_m$ and $x > x_m$ respectively. Because of the P^{-1} integration kernel, $g_m(x)$ changes abruptly at the maxima adjacent to the minimum of the potential at x_m. These functions are put to be zero outside the range of definition, and they obey the condition

$$\sum_{m=1}^{M} g_m(x) = 1 \tag{4}$$

Note that the localized functions $g_m(x)P(x)$ satisfy the equation

$$\hat{R}P(x)g_m(x) = 0, \tag{5}$$

i.e. they behave locally as eigenfuctions of the diffusion operator with a vanishing eigenvalue, like the distribution $P(x)$ itself.

Within this reduced set of functions we construct overlap matrix elements S_{mn}

$$S_{mn} = \int dx g_m(x)P(x)g_n(x) = \langle g_m|P|g_n\rangle \tag{6}$$

matrix elements of the diffusion operator R_{mn}

$$R_{mn} = \langle g_m|R|P_{g_n}\rangle \tag{7}$$

and the equilibrium site populations Q_m

$$Q_m = \langle g_m|P\rangle = \sum_n S_{mn}. \tag{8}$$

We then proceed to define the projection operator $\mathcal{P}$, which allows us to find eigensolutions of the diffusion operator $\hat{R}$ on the subspace spanned by the site functions g_m

$$\mathcal{P}P(x)f(x) = P(x)\sum_m g_m(x)f_m, \tag{9}$$

where

$$f_m = \sum_n (S^{-1})_{mn}\langle g_n|P|f\rangle \tag{10}$$

has to be interpreted as the 'site value' of the function *f(x)*, corresponding to the *m*th site. With these ingredients, we are able to describe the time

evolution of the site probability $P_m(t)$ by applying the projection operator techniques [15, 16]

$$P_m(t) = \langle g_m | P(x,t) \rangle, \tag{11}$$

$$(\partial/\partial t) P_m(t) = -\sum_n W_{mn} P_n(t), \tag{11'}$$

with $\mathbf{W} = \mathbf{RS}^{-1}$. Alternatively, we can calculate the correlation function directly for any function *f(x)*, through the relation

$$\overline{f(t)^* f} = \mathbf{f}^\dagger \exp(-\mathbf{W}t)\mathbf{Sf} \tag{12}$$

f being a column vector of elements f_m.

For very steep distributions,

$$P(x) \simeq \sum_m Q_m \delta_m(x), \tag{13}$$

with $\delta_m(x)$ a delta function centred at x_m, $g_m(x)$ tends to a square function with a value of unity in the domain between the two maxima adjacent to the minimum of the potential at x_m, and the off-diagonal elements of the overlap matrix can be neglected. Under these limiting conditions:

$$f_m \simeq f(x_m), \tag{14}$$

$$S_{mn} \simeq Q_m \delta_{mn}. \tag{14'}$$

In particular, if a parabolic expansion of the potential is performed in equation (8) about the position of each minimum, the site populations Q_m can be expressed as

$$Q_m = \exp(-E_m/kT) \Big/ \sum_m \exp(-E_m/kT), \tag{15}$$

with the 'free energy' E_m given by [25]

$$E_m = V_m + (kT/2)\ln(V_m^{(2)}/2\pi kT) \tag{16}$$

and the 'entropy' term determined by the potential curvature given by the second derivative $V_m^{(2)}$ calculated at $x = x_m$. The average of a function *f(x)* therefore becomes:

$$\begin{aligned} \bar{f} &= \int dx P(x) f(x), \\ &= \sum_m f_m Q_m. \end{aligned} \tag{17}$$

The jump matrix **W** is tridiagonal when off-diagonal elements of the overlap matrix **S** are neglected, the integrand in equation (7) for $R_{m,m+1}$ being

non-vanishing only in the range (x_m, x_{m+1}) of common definition of the adjacent site functions g_m and g_{m+1}. A simple expression of these two functions in the range (x_m, x_{m+1}) is easily obtained if a parabolic expansion of the potential is performed about the saddle point x_s dividing the two domains pertaining to the minima at x_m and x_{m+1}

$$V(x) = V_s - (1/2)|V_s^{(2)}|(x - x_s)^2. \tag{18}$$

Note that the potential curvature is negative at x_s. Insertion of this result into equation (3) gives, after the variable change $y = x - x_s$ and extension of the integration limits to infinity:

$$g_m(y) = 1/2 - (|V_s^{(2)}|/2\pi kT)^{1/2} \int_0^y dz \exp(z^2 V_s^{(2)}/2kT), \tag{19}$$

$$g_{m+1}(y) = 1/2 + (|V_s^{(2)}|/2\pi kT)^{1/2} \int_0^y dz \exp(z^2 V_s^{(2)}/2kT). \tag{19'}$$

Again, using a similar expansion of the integrand in equation (7), one finally obtains for the jump matrix element $W_{m,m+1}$

$$\begin{aligned} W_{m,m+1} &= \langle \partial g_m/\partial x | D(x) P(x) | \partial g_{m+1}/\partial x \rangle / Q_{m+1} \\ &\simeq -(D_s|V_s^{(2)}|/2\pi kT) \exp\{-(E_s - E_{m+1})/kT\}, \end{aligned} \tag{20}$$

with E_s corresponding to the free energy of the saddle point

$$\exp(-E_s/kT) = (|V_s^{(2)}|/2\pi kT)^{-1/2} \exp(-V_s/kT) \tag{21}$$

and D_s denoting the diffusion coefficient for the conformation assumed at the saddle point. In this way the Kramers expression for jump rates in the overdamped regime is recovered.

We shall now generalize these results to multidimensional problems, for which it is still possible to write down a diffusion equation in the form of equation (1) for the probability density $P(\mathbf{x}, t)$, with

$$\mathbf{x} = \{x_1, x_2, \ldots, x_N\} \tag{22}$$

and

$$\hat{R} = -(\partial/\partial \mathbf{x})^{\dagger} \mathbf{D}(\mathbf{x}) P(\mathbf{x}) (\partial/\partial \mathbf{x}) P(\mathbf{x})^{-1}. \tag{23}$$

To derive an expression for the jump matrix elements W_{mn}, we consider two local minima m, n of the multidimensional potential $V(\mathbf{x})$, connected through a single saddle point s, and we denote by $\mathbf{V}_m^{(2)}$, $\mathbf{V}_n^{(2)}$ and $\mathbf{V}_s^{(2)}$ the matrices of the second derivatives of the potential, calculated at $\mathbf{x}_m$, $\mathbf{x}_n$ and $\mathbf{x}_s$ respectively. From the geometry of the problem, it follows that $\mathbf{V}_m^{(2)}$ and $\mathbf{V}_n^{(2)}$ possess only positive eigenvalues, whereas $\mathbf{V}_s^{(2)}$ has a unique negative eigenvalue.

Equipped with these definitions, we obtain the equivalent of the free energy given in equation (16) as

$$E_m = V_m + (kT/2)\ln|\mathrm{Det}(\mathbf{V}_m^{(2)}/2\pi kT)| \tag{24}$$

where $V_m = V(\mathbf{x}_m)$. By a parabolic expansion about the saddle point $\mathbf{x}_\mathrm{s}$ of the potential in the diffusion operator, we then obtain from equation (5):

$$\begin{aligned}(\partial/\partial\mathbf{x})^\dagger\mathbf{D}(\mathbf{x})P(\mathbf{x})(\partial/\partial\mathbf{x})g_m(\mathbf{x}) \\ &\simeq (\partial/\partial\ \delta\mathbf{x})^\dagger\mathbf{D}_\mathrm{s}\exp(-\delta\mathbf{x}^\dagger\mathbf{V}_s^{(2)}\delta\mathbf{x}/2kT)(\partial/\partial\ \delta\mathbf{x})g_m \\ &= 0\end{aligned} \tag{25}$$

with

$$\delta\mathbf{x} = \mathbf{x} - \mathbf{x}_\mathrm{s} \tag{26}$$

and $\mathbf{D}_\mathrm{s}$ the value of the N-dimensional diffusion tensor for the geometry corresponding to $\mathbf{x}_\mathrm{s}$.

The matrix product $\mathbf{D}_\mathrm{s}\mathbf{V}_\mathrm{s}^{(2)}$ can be put into a diagonal form by the transformation

$$\mathbf{S}^{-1}\mathbf{D}_\mathrm{s}\mathbf{V}_\mathrm{s}^{(2)}\mathbf{S} = kT\wedge \tag{27}$$

and so through the change of variable

$$\mathbf{y} = \mathbf{S}^{-1}\ \delta\mathbf{x} \tag{28}$$

the operator acting on g_m is factorized

$$\sum_j(\partial/\partial y_j)\exp(-\lambda_j y_j^2/2)(\partial/\partial y_j)g_m = 0. \tag{29}$$

Let the unique negative eigenvalue of equation (27) be denoted by λ_1. The associated eigenvector represents the most probable direction of crossing the saddle point amongst all the trajectories joining the adjacent minima, and the coordinate y_1 is the displacement along such a direction. The differential equation (29) is readily solved by assuming that g_m depends upon the coordinate y_1 only, and an error function shape as in equation (19) is thus obtained:

$$g_m(y_1) = (1/2) \pm (|\lambda_1|/2\pi)^{1/2}\int_0^{y_1} dz\ \exp(z^2\lambda_1/2). \tag{30}$$

The positive or negative sign has to be taken according as to whether the minimum $\mathbf{x}_m$ is reached by increasing or decreasing values of y_1. An analogous relation with opposite sign of the integral holds for the localized function g_n associated with the adjacent minimum $\mathbf{x}_n$, near the same saddle

point $\mathbf{x}_s$. The transition rate W_{mn} is then obtained by performing a local expansion of the integrand as in equation (20) 235

$$W_{mn} = -(|\lambda_1|/2\pi)\exp\{-(E_s - E_n)/kT\} \tag{31}$$

an expression analogous to equation (24) is used to define the free energy E_s of the saddle point. Note that the free energy E_m does not appear, since W_{mn} represents the kinetic rate for the transition $n \rightarrow m$. The result given by equation (31) is the generalization to the multivariate problem of the Kramers theory as found by Langer [10], and this confirms the consistency of the site functions set.

Relation (31) holds for the off-diagonal elements of **W**, provided that a saddle point connects the domains relative to the minima located at $\mathbf{x}_m$ and $\mathbf{x}_n$. Off-diagonal elements of **W** corresponding to pairs of sites not directly connected by a saddle point, are taken to be zero because of the unfavourable energetics of the transition, while the diagonal terms are determined by the condition that **Q** is the stationary solution of **W**

$$W_{mm} = -Q_m^{-1}\sum_{n\neq m} W_{mn}Q_n. \tag{32}$$

3. THE MODEL FOR ALIPHATIC TAILS

In the following we shall consider a molecular system composed of a flexible chain attached to a rigid core whose motion is neglected for the moment; later on we shall take it into account by convoluting the correlation functions for the internal and the overall rotations. In order to define a particular geometry of the chain, an axis system centered on each rotating methylene carbon atom is chosen in the following way. The z_i axis of the cartesian frame M_i centred on C_i is directed along the $C_i - C_{i+1}$ bond direction, and the x_i axis lies in the plane $C_{i-1} - C_i - C_{i+1}$ of the carbon-carbon bonds. Note that this choice differs from that adopted by Flory [1]. We shall then denote by $\mathbf{\Omega}_i = (\alpha_i,\ \beta_i,\ \gamma_i)$ the set of Euler angles, chosen according to the convention of Rose [26], that brings the axis system M_{i-1} into coincidence with M_i. More specifically, $\mathbf{\Omega}_i$ will have the form

$$\mathbf{\Omega}_i = (\alpha_i,\ 180^\circ - \delta_c,\ 180^\circ) \tag{33}$$

with α_i the rotation angle about the $C_{i-1} - C_i$ carbon–carbon bond, and δ_c the angle between consecutive bonds of the chain. We suppose also that the chain is attached to a 'ghost' methylene group labelled as C_0, which is considered part of the rigid core. In this way, the set of Euler angles $\mathbf{\Omega}_1$ is unambiguously defined as the orientation of M_1 with respect to the cartesian frame M_0, which in turn could be used to specify the orientation

of the rigid core with respect to a laboratory frame. The rotation of the terminal methyl group about the threefold symmetry axis will not be considered because such a motion is not expected to be correctly described by the model we propose here. Therefore, the aliphatic tails treated here will be specified by the number N of methylene-methylene bonds, the conformational dynamics being described in terms of the N torsional angles $\alpha_1, \alpha_2, \ldots, \alpha_N$.

Before considering in detail the energetics of the conformational transitions, the geometry-dependent interactions between rigid core and chain must be modelled. In order to deal with a standard and simple form of the internal potential, we assume that the contribution to the conformational energy of the mobile chain from the rigid core comes uniquely from the ghost C_0 group. In other words, the internal potential $V(\alpha_1, \alpha_2, \ldots, \alpha_N)$ for a chain constrained at one end, and characterized by N torsional angles, is considered to be the same of that of a free normal alkane composed of $N+3$ carbon atoms. Let us consider, to begin with, the case $N = 1$ of the butane molecule. According to the torsional potential calculated by Scott and Scheraga [27] and parameterized by Ryckaert and Bellemans [28], the minima are located at $\alpha_1 = 0,\ \pm 120^\circ$ for the trans (t) and the gauche ($g_\pm$) states, with the two saddle points for the transitions $t \rightleftharpoons g_\pm$ at $\alpha_1 = \pm 60^\circ$. At any given temperature T, one can calculate the free energies E_t and E_g of the stable conformers and the energy E_s of the saddle points, according to equations (16) and (21). The same procedure can be applied in principle to any chain, but this requires the analytical form of the internal potential as a function of the N torsional angles α_i. The alternative is represented by a parametrization of geometry and energetics of the stable conformers, taking into account in a simple form all prominent features of the interactions between methylene groups. The model used in the calculations is defined by the following rules:

(i) The geometry of each stable conformer is specified by a sequence of conformational states t or $g_\pm$ characterized by the same torsional angles α_i of a butane molecule.

(ii) The free energy of a given conformation can be decomposed into two terms: the sum of independent contributions E_t or E_g of each torsional degree of freedom, and the increment of the free energy caused by the 'pentane effect' [1], given by a quantity ΔE_p multiplied by the number of sequences $g_\pm g_\mp$ occurring in the chain.

(iii) If d_{ca} denotes the distance of closest approach between carbon atoms separated by at least four bonds, any acceptable configuration must obey the condition:

$$|\mathbf{r}_j - \mathbf{r}_k| \geq d_{ca}, \quad \text{for } |j-k| > 4, \tag{34}$$

$\mathbf{r}_j$ being the vector position of the jth carbon atom. This condition excludes states with an unphysical overlap of the methylene groups.

The parametrization of the geometry and the energetics of the saddle points are now required in order to calculate the elements of the transition matrix $\mathbf{W}$. If we neglect multiple bond transitions because of their unfavourable activation energy [8, 9], the elements of $\mathbf{W}$ connect only conformations differing by the value of a single torsional angle. Let us consider the saddle point corresponding to the $n \rightarrow m$ transition, obtained by rotating the k-th bond. The geometrical structure of the chain at the saddle point is obtained from the nth equilibrium conformation by changing the α_k torsional angle by 60°. This is equivalent to 'factorizing' the geometrical structure of the chain according to rule (i). The corresponding free energy E_s is defined by the single parameter ΔE_s taken as the increment of E_s with respect to the energy of the starting or of the final conformation, whichever is larger:

$$E_s = \Delta E_s + \mathrm{Max}(E_m, E_n). \tag{35}$$

To implement the theoretical result given in equations (27) and (31), the diffusion matrices must now be calculated for all saddle points connecting adjacent minima of the potential. We shall adopt a simple bead model, by regarding each methylene group as a sphere centered at the carbon positions, according to a standard assumption of BD trajectory calculations for alkyl chains [11, 12]. This approximation is certainly crude, but it is expected to give a realistic description of the frictional effects; any more accurate estimate of these effects can be incorporated into the present scheme. We recall first that the diffusion tensor $\mathbf{D}$ can be written as $kT\boldsymbol{\xi}^{-1}$, $\boldsymbol{\xi}$ being the friction tensor defined by the relation $\mathbf{N} = -\boldsymbol{\xi}.\boldsymbol{\omega}$ where the torque $\mathbf{N}$ causes the damping of the angular velocity $\boldsymbol{\omega}$ of a rotating body.

A similar relation can be written for the torsional motions of the chain, by identifying the kth component of the N-dimensional arrays $\boldsymbol{\omega}$ and $\mathbf{N}$ with the torsional velocity $\omega_k = \dot{\alpha}_k$ and the torque N_k opposing the rotation about the kth bond, respectively. The friction matrix $\boldsymbol{\xi}$ can be easily derived if we suppose that the torsional degrees of freedom are uncoupled with the overall rotation of the entire molecule. This assumption is justified when dealing with massive rigid cores whose rotational diffusion does not affect the conformational transitions. Since the rotation about the $C_{k-1} - C_k$ bond causes translations of all beads numbered from $k + 1$ to $j = N + 1$, the latter denoting the terminal methyl group, the torque N_k is calculated to be:

$$N_k = \mathbf{z}_{k-1} \cdot \left[\sum_{j=k+1}^{N+1} (\mathbf{r}_j - \mathbf{r}_k) \times \mathbf{F}_j \right] \tag{36}$$

where $\mathbf{z}_{k-1}$ is the unit vector pointing in the direction of the $C_{k-1} - C_k$ bond, and $\mathbf{F}_j$ is the viscous drag for the translational motion of the jth sphere given by the Stokes–Einstein law

$$\mathbf{F}_j = -\xi_0 \mathbf{v}_j \tag{37}$$

$$\xi_0 = 4\pi R\eta. \tag{37'}$$

In the last expression, R is the radius of the spheres which are assumed to be all equal, and η is the viscosity of the medium. Slip boundary conditions are considered to be consistent with the neglect of the intrinsic frictional torque for the rotation of each bead about its own axis. The linear velocities $\mathbf{v}_j$ are related to the torsional velocities by the expression

$$\mathbf{v}_j = \sum_{i=1}^{j-1} \omega_i \mathbf{z}_{i-1} \times (\mathbf{r}_j - \mathbf{r}_i) \tag{38}$$

and therefore the relation $\mathbf{N} = -\boldsymbol{\xi}\boldsymbol{\omega}$ is recovered with the elements of the friction matrix given as

$$\xi_{ki} = \xi_0 \sum_{j=j'}^{N+1} [\mathbf{z}_{k-1} \times (\mathbf{r}_j - \mathbf{r}_k)].[\mathbf{z}_{i-1} \times (\mathbf{r}_j - \mathbf{r}_i)], \tag{39}$$

j' being the largest of the integers $(k + 1)$ and $(i + 1)$. For each transition $n \rightarrow m$, the matrix $\boldsymbol{\xi}$ is calculated given the geometry of the saddle point and the distance d between two adjacent carbon atoms.

In order to calculate from equation (27) the negative eigenvalue λ_1 which determines the pre-exponential factor in the transition rate W_{mn} of equation (31), knowledge of the curvature matrix $\mathbf{V}_s^{(2)}$ at the saddle point is also required. Even if the curvatures could be obtained in principle from the analytical form of the internal potential, we shall use again a simple parametrization procedure. The $\mathbf{V}_s^{(2)}$ matrix is assumed to be diagonal with respect to the displacements of the torsional angles α_i, with a unique positive curvature $V_{nr}^{(2)}$ for all the 'non-reactive' modes, except for a negative curvature $V_r^{(2)}$ for the 'reactive' mode α_k modified by the single bond transition $n \rightarrow m$.

Note that in the case of a single degree of internal freedom, only one friction coefficient can be evaluated: $\xi = \xi_0 d^2$, d being the carbon-carbon bond length. For this case, the $g \rightarrow t$ isomerization rate w is obtained from equation (20) as

$$w = (|V_r^{(2)}|/2\pi d^2 \xi_0) \exp(-\Delta E_s/kT). \tag{40}$$

It is therefore convenient to express the jump matrix elements W_{mn} in terms of w, which will appear in the numerical calculations as a scaling factor. In order to do so, we first symmetrize the jump matrix $\mathbf{W}$

$$\mathbf{W}^{\mathrm{s}} = \mathbf{S}^{-1/2}\mathbf{W}\mathbf{S}^{1/2} = \mathbf{W}^{\mathrm{s}\dagger}. \tag{41}$$

The elements of the symmetrized matrix $\mathbf{W}^{\mathrm{s}}$ are then

$$W^{\mathrm{s}}_{m,n} = -(w/|\mu_1|)\exp\{-|E_m - E_n|/2kT\}, \tag{42}$$

with the purely numerical factor μ_1 given as

$$\mu_1 = |V_{\mathrm{r}}^{(2)}|/d^2\xi_0\lambda_1. \tag{43}$$

From equation (27), one derives that μ_1 can be alternatively defined as the unique negative eigenvalue of the following matrix

$$\mathbf{M} = (\mathbf{V_s}^{(2)-1}|V_{\mathrm{r}}^{(2)}|)(\boldsymbol{\xi}/\xi_0 d^2), \tag{44}$$

where the friction coefficients are scaled by the factor $\xi_0 d^2$. Because of the $|V_{\mathrm{r}}^{(2)}|$ scaling of the $\mathbf{V_s}^{(2)}$ matrix, only the knowledge of the ratio ρ of the curvatures for the reactive and non-reactive modes

$$\rho = |V_{\mathrm{r}}^{(2)}|/V_{\mathrm{nr}}{}^{(2)} \tag{45}$$

is required, instead of their absolute values. Note that when $\rho = 0$, the eigen value μ_1 becomes equal to $|\mu_1| = \xi_{kk}/\xi_0\, d^2$, the index k denoting the specific C-C bond involved in the transition. A vanishing value of ρ implies very steep slopes of the potential surface for the non-reactive modes, which hinder any cooperative effect [8, 9]. In fact, ξ_{kk} is simply the friction opposing the motion of the beads labelled from $(k+1)$ to $(N+1)$, when displaced all together by the single rotation about the $\mathrm{C}_{k-1} - \mathrm{C}_k$ bond.

We conclude this section by noting that the calculations of equilibrium distributions and transition rate coefficients ultimately require four independent parameters: the rate w for the conformational transitions of the terminal group, the ratio ρ of the potential curvatures, and the two scaled energy parameters e_g and e_p defined as

$$e_g = (E_g - E_t)/kT, \tag{46}$$

$$e_g = \Delta E_p/kT. \tag{46'}$$

These parameters represent the smallest set necessary to characterize in a realistic way the conformational dynamics of the chains.

4. COMPUTATIONAL METHODS

In the previous sections, the physical model has been completely specified by defining the geometry of the chain, the equilibrium distribution of the conformations and the microscopic kinetic rates. We shall now describe in

some detail how to implement the model for the calculation of the spectral densities of correlation functions associated with specific observables.

An ensemble of indices $J = \{j_1, j_2, \ldots, j_N\}$, with $j_i = 0, \pm 1$ corresponding to the t and $g_\pm$ states respectively, is required to specify completely the conformational state of a chain with N segments. For a given J, the energy in units of kT of the corresponding conformer is calculated in terms of the two parameters e_g and e_p defined in equation (46) and equation (46′), as

$$e_J = n_g e_g + n_p e_p, \tag{47}$$

where n_g is the number of gauche states and n_p is the number of sequences $g_\pm\, g_\mp$. The site equilibrium population defined in equation (15) becomes

$$Q_J = \exp\,(-e_J) \Big/ \sum_J \exp\,(-e_J) \tag{48}$$

where the summation runs over all the allowed conformations.

In order to specify the geometry of a given conformer, we introduce the Euler matrix $\mathbf{E}_i$ which rotates the components of a give vector from the M_{i-1} frame to the M_i frame centered on the ith methylene group. From the set of Euler angles Ω_i defined in equation (33), the following explicit form of $\mathbf{E}_i$ is derived.

$$\mathbf{E}_i = \begin{vmatrix} \cos\,\delta_c\,\cos\,\alpha_i & \cos\,\delta_c\,\sin\,\alpha_i & \sin\,\delta_c \\ \sin\,\alpha_i & -\cos\,\alpha_i & 0 \\ \sin\,\delta_c\cos\,\alpha_i & \sin\,\delta_c\sin\,\alpha_i & -\cos\,\delta_c \end{vmatrix}, \tag{49}$$

with α_i determined by the ith index of J

$$\alpha_i = 2\pi j_i/3. \tag{50}$$

In order to implement the condition of closest approach given in equation (34), the components $\mathbf{s}_{i,k}$ in the M_i frame of the vector $(\mathbf{r}_k - \mathbf{r}_i)/d$ are calculated from the recursive relation

$$\mathbf{s}_{i,k} = \mathbf{s}_1 + \tilde{\mathbf{E}}_{i+1}\,\mathbf{s}_{i+1,k}, \tag{51}$$

with $\mathbf{s}_{k,k} = 0$ and $\mathbf{s}_1 = \mathbf{s}_{i,i+1} = (0,\ 0,\ 1)$. Unless otherwise stated, the following geometrical parameters have been used in the calculations: $\delta_c = 112^\circ$, $d = 1{\cdot}53\,\text{Å}, \mathrm{d_{ca}} = 2\,\text{Å}$. The value of d_{ca} has been chosen to be small enough to eliminate only strongly overlapping conformations. The shortest sequence excluded in this way is $g_\pm g_\mp g_\pm$, corresponding to a cyclohexane molecule in the chair conformation with a broken C-C bond, the distance between the terminal methylene groups being comparable to the C-C bond length. The next forbidden sequence is $g_\pm g_\pm g_\mp g_\mp g_\pm$, and some more appear in the $N = 7$ chain.

After exclusion of the forbidden sequences, the number N_c of allowed conformations is sensibly reduced from the total number of 3^N possible configurations. For example, N_c is reduced to 197 from 243 for the $N = 5$ chain, while for the $N = 7$ chain we obtain $N_c = 1552$ compared to 2187 starting conformations.

The number of allowed conformations grows very quickly with increasing chain length even after exclusion of the forbidden sequences. To obtain matrices manageable in medium size computers we require a further reduction of the dimension N_c, by excluding conformers with Boltzmann factors $\exp(-e_J)$ less than a cutoff value q_0 [29]. This is equivalent to neglecting the contribution of conformations with a relative equilibrium population less than q_0 with respect to the all-trans chain. Of course this procedure is necessary only for long chains; the $N = 5$ chain can be treated without any truncation, and it has been used to test which values of q_0 provide results within an accuracy of 0·1 per cent for both static properties (averages of angular functions) and dynamic observables (spectral densities). A reasonable value of the cutoff parameter is $q_0 = 10^{-3}$, which allows a reduction to $N_c = 953$, for an $N = 7$ chain, when the following values of the energy parameters are used: $e_g = 0.84, e_p = 3$.

We shall now describe the method for the calculation of the symmetrized rate matrix with elements $W^{\mathrm{s}}_{J'J''}$. Since only single bond transitions are considered, final and starting conformations must satisfy the following 'selection rule', in order to have non-vanishing off-diagonal elements:

$$|j'_k - j''_k| = 1, \text{ and } j'_i = j''_i \text{ for } i \neq k, \tag{52}$$

where k gives the position of the rotating bond. Note that direct conversion between gauche states is not allowed, because of the very high energy barrier [15].

As in the case of stable conformers, we introduce a set of indices $J \equiv \{j_1, j_2, \ldots, j_i, \ldots, j_N\}$ to describe the transition state with a half-integral value for the rotating bond

$$j_i = (j'_i + j''_i)/2. \tag{53}$$

In this way, the previous definitions of the Euler matrices $\mathbf{E}_i$ and of the arrays $\mathbf{s}_{i,k}$ also apply to the geometrical description of the saddle points. The friction matrix defined in equation (39), after scaling by the factor $\xi_0 d^2$, is calculated from the following expression:

$$\xi_{mn}/\xi_0 d^2 = \sum_{i=i'}^{N+1} [(\mathbf{s}_{m-1,i})_1 (\mathbf{s}_{n-1,i})_1 + (\mathbf{s}_{m-1,i})_2 (\mathbf{s}_{n-1,i})_2], \tag{54}$$

with i' the largest of the two integers $(m + 1)$ and $(n + 1)$.

The recursive relation (51) allows a very efficient calculation of the scaled friction matrix. In practice, the ensemble of arrays $\mathbf{s}_{m,n}$ are computed and stored for a given value of the index n, all elements of the friction matrix are augmented by the corresponding contribution defined by equation (54), and the procedure is repeated for the next value of the index n. The matrix $\mathbf{M}$ defined in equation (44) is then calculated, and using the EISPACK [30] diagonalization routine for real matrices, the negative eigenvalue μ_1 which appears in the pre-exponential factor of equation (42), is derived.

Because of the repeated calculations of the friction matrix and the diagnolizations of $\mathbf{M}$ for all the active transitions, the computation of $\mathbf{W}^s$ turns out to be rather time-consuming. It is therefore convenient to calculate $\mathbf{W}^s$ once and for all, given a set of parameters e_g, e_p, w and ρ, and to store it in a disk file to be recalled in the calculations of different types of observables.

The ultimate goal of this computation is the evaluation of correlation functions, using equation (12) for any given function f of the torsional angles $\alpha_1, \alpha_2, \ldots, \alpha_N$. The elements f_J of the vector $\mathbf{f}$, are easily calculated according to equation (14) from the values of the torsional angles given in equation (50). Actually, the computed quantities, are the spectral densities $\tilde{G}(\omega)$ of the correlation functions, because they describe directly the spectroscopic observables. It is convenient to examine the deviation δf of the function from its average $\bar{f}$, in order to avoid the divergence of $\tilde{G}(\omega)$ for $\omega = 0$. In conclusion, the spectral densities are calculated according to the following equations:

$$\tilde{G}(\omega) = \mathbf{v}^\dagger (i\omega \mathbf{I} + \mathbf{W}^s)^{-1} \mathbf{v}, \tag{55}$$

$$v_J = Q_J^{1/2} (f_J - \bar{f}), \bar{f} = \mathbf{Q}^\dagger \mathbf{f} \tag{55'}$$

and their dependence upon the frequency is expressed by the continued fraction representation generated by the Lanczos algorithm [31, 32] applied to the real symmetric matrix $\mathbf{W}^s$ with $\mathbf{v}$ as starting vector.

Of course, one can use alternative methods, such as the full diagonalization of the matrix $\mathbf{W}^s$. However, efficient algorithms are required because of the size of the matrix for large N, and the necessity of calculating many spectral densities corresponding to physical properties observed at different carbon positions. The Lanczos algorithm represents a natural choice when dealing with highly sparse matrices [33]. This is our case, since the number of non-zero elements for each row of $\mathbf{W}^s$ is proportional to N, while the dimension N_c of the matrix grows exponentially with N. Another reason for choosing the Lanczos algorithm is that the number of coefficients of the calculated continued fraction representation

are usually much less than the dimension of the matrix. In our problems, $N_c/20$ iterations of the Lanczos algorithm turn out to be sufficient. As a conclusion, a reasonably short time is required to compute spectral densities for chains of relatively high complexity. For example, for the $N = 7$ chain with $N_c = 953$, each spectral density requires about 30 minutes CPU time on a PDP 11-24 minicomputer.

5. OBSERVABLES AND CORRELATION FUNCTIONS

The physical observables we are interested in are the electric dipole and magnetic dipole or quadrupole interactions, described in terms of first and second rank tensors, respectively. Molecular systems particularly suitable to the present theoretical analysis are the tetrahexyl- or tetraoctylammonium ion salts [34], which provide a simple example of effective time scale separation between the segmental motion and the overall rotation of the molecule, the constrained end of the chain being immediately identified with the nitrogen core. More interesting objects are the phospholipid membranes, characterized by relatively immobilized polar heads and flexible chains, which have been subjected to detailed investigations [35], even if in this case the effect of intermolecular potentials should be incorporated in our theoretical model.

Observation of electric dipole relaxation implies the presence of bonds with strong dipolar character, and in fact experimental data on the complex dielectric permittivity are reported for liquid octyl iodide [36]. In this case, the chain is free and the present treatment could not be applied, unless it is permissible, at least as a rough approximation, to identify a 'centre of constraint' localized in the middle of the chain. The most numerous observations however refer to selective N.M.R. carbon-13 or deuteron relaxation [3–5, 35, 37]. In both cases, the relaxation mechanism is related to the fluctuations of a second rank tensor which is generally considered to be axially symmetric about the C-H bond direction. Expressions for the relevant interactions and the spin relaxation times are reported in [5].

In order to describe dielectric or magnetic relaxation, we need to calculate correlation functions of Wigner rotation matrices relating the local interaction frame $\boldsymbol{F}$ to the laboratory system $\boldsymbol{L}$. At first, we shall perform the transformation to a diffusion frame $\boldsymbol{D}$ of the core in which the diffusion tensor is diagonal, that does not necessarily coincide with the frame $\boldsymbol{M}_0$ of the 'ghost' methylene group.

When we are interested in the motion of the frame $\boldsymbol{F}$ attached to the nth methylene carbon atom, the relevant Wigner functions to be calculated are

$$D^j_{q0}(\Omega_{\mathrm{LF}}) = \sum_{p,\ b_0,\ b_n} D^j_{qp}(\Omega_{\mathrm{LD}}) D^j_{pb_0}(\Omega_{\mathrm{D}0}) D^j_{b_0 b_n}(\Omega_{0n}) D^j_{b_n 0}(\Omega_{nF}) \tag{56}$$

where the angles $\Omega_{\mathrm{D}0}$ and Ω_{nF} are time independent, and the internal motions only affect the angles Ω_{0n} relating the orientation of the M_n frame to M_0.

If the internal motions are assumed to be uncoupled to the rotational diffusion of the whole molecule, described by the correlation functions $C^{j(D)}_{qp}(t)$ of the Wigner rotation matrix components $D^j_{qp}(\Omega_{\mathrm{LD}})$, then the correlation function for the motion of the interaction tensor component along the C_n-H bond is expressed by the product

$$G^{j(n)}_{q0}(t) = \sum_p C^{j(D)}_{qp}(t) G^{j(\mathrm{int})}_{p0}(t), \tag{57}$$

where $G^{j(\mathrm{int})}_{p0}(t)$ is the correlation function of $D^j_{p0}(\Omega_{\mathrm{DF}})$, implicitly defined in equation (56).

In general, due to the presence of the conformational potential, the following expression holds:

$$G^{j(int)}_{p0}(t) = |\overline{D^j_{p0}}|^2 + \delta G^{j(\mathrm{int})}_{p0}(t), \tag{58}$$

with $\delta G^{j(\mathrm{int})}_{p0}(t)$ the correlation function for the deviation of $D^j_{p0}(\Omega_{\mathrm{DF}})$ from the equilibrium average $\overline{D^j_{p0}}$, whose non-vanishing value is a measure of the degree of spatial restriction of the segmental motions [37].

The computational programs are designed to handle the most general cases, but it is convenient here to remove unnecessary complications in the presentation of the physically relevant results. Therefore we shall consider isotropic diffusion, and after eliminating some redundant indices equation (57) reduces to

$$G^j_n(t) = (2j+1)^{-1} \exp\,[-j(j+1)Dt]\{(S^j_n)^2 + [1-(S^j_n)^2] g^j_n(t)\}, \tag{59}$$

with

$$(S^j_n)^2 = \sum_p |\overline{D^j_{p0}}|^2 \tag{60}$$

and

$$g^j_n(t) = \sum_p \delta G^{j(\mathrm{int})}_{p0}(t) / \sum_p \delta G^{j(\mathrm{int})}_{p0}(0). \tag{61}$$

In this way, S^j_n is a generalized order parameter for the nth segment and $g^j_n(t)$ is a normalized relaxation function for 'reduced' tensorial quantities of rank j associated to that segment. Here the term 'reduced' is used in the sense that no reference to a specific tensor component is made.

The spectral density $\tilde{G}_n^j(\omega)$ of the correlation function $G_n^j(t)$ is finally given by the relation

$$\tilde{G}_n^j(\omega) = (2j+1)^{-1}\{(S_n^j)^2/[i\omega + Dj(j+1)] + [1-(S_n^j)^2]\tilde{g}_n^j[\omega - iDj(j+1)]\}, \quad (62)$$

where $\tilde{g}_n^j(\omega)$ is the spectral density of the correlation function for internal motions $g_n^j(t)$. The zero-frequency value $1/\tilde{g}_n^j(0) = k_n^j$ can be interpreted as a characteristic relaxation rate for reduced tensorial quantities of jth rank associated to the nth segment of the chain.

The spectral density $\tilde{g}_n^j(\omega)$ for the internal motions can be expressed according to equation (61) as a linear combination of spectral densities associated with the functions $D_{p0}^j(\Omega_{\mathrm{DF}})$, each of them being evaluated by the method discussed in the previous section. In particular, we need to calculate the N_c-dimensional array $\mathbf{D}_{p0}^j$ having as elements the values of $D_{p0}^j(\Omega_{\mathrm{DF}})$ in correspondence of the allowed conformations. This is not a trivial computational task for a chain with a large number of conformations. One possibility is to decompose $D_{p0}^j(\Omega_{\mathrm{DF}})$ as

$$D_{p0}^j(\Omega_{\mathrm{DF}}) = \sum_{b_0,b_1,b_2\ldots b_N} D_{pb_0}^j(\Omega_{\mathrm{D}0}) D_{b_0b_1}^j(\Omega_1) D_{b_1b_2}^j(\Omega_2) \ldots D_{b_{n-1}b_n}^j(\Omega_n) D_{b_n0}^j(\Omega_{nF}), \quad (63)$$

with the Euler angles $\Omega_i \equiv \Omega_{i-1,i}$ calculated for each conformation according to equation (33). Alternatively, the Euler matrix E_{FD} which rotates the components of a vector from the D-frame to the F-frame, is computed for any given conformation

$$\mathbf{E}_{\mathrm{FD}} = \mathbf{E}_{\mathrm{F}n}\mathbf{E}_n \ldots \mathbf{E}_2\mathbf{E}_1\mathbf{E}_{\mathrm{OD}}, \quad (64)$$

with $\mathbf{E}_i \equiv \mathbf{E}_{i,i-1}$ given explicitly by equation (49), and the Euler angles Ω_{DF} specifying the elements of $\mathbf{E}_{\mathrm{FD}}$ are used to compute the corresponding values of $D_{p0}^j(\Omega_{\mathrm{DF}})$. We have found the second procedure to be generally more convenient, because the number of operations does not increase with the rank of the function to be evaluated. The final spectral densities are calculated according to equation (55), by identifying $\mathbf{f}$ with $\mathbf{D}_{p0}^j$, and the order parameter are calculated as

$$S_n^j = \left(\sum_p |\mathbf{Q}^\dagger \mathbf{D}_{p0}^j|^2\right)^{1/2}. \quad (65)$$

Apart from first-rank electric dipole and second rank magnetic interactions, there are other properties of relevant physical interest even if they do not have an unambiguous mathematical definition, i.e. the kinetic rates for the conformational isomerization of each chain segment. In the case of

the butane molecule, with a unique degree of internal freedom, the vectors $(-1, 2, -1)$ and $(1, 0, -1)$ relative to the conformational states (g_+, t, g_-) are eigenvectors of the $\mathbf{W}$ matrix, with eigen-values $K_g + 2K_t$ and K_g respectively, where K_g and K_t are the forward and backward kinetic rates for the reaction $g \rightleftharpoons t$ [12, 15]. These eigenvalues can be interpreted as the kinetic rates for the decay of excess trans populations or unbalanced gauche populations, respectively. We might therefore generalize these concepts to chains of N segments, by defining the vectors $\mathbf{P}_n^t$ of components $[\mathbf{P}_n^t]_J = (3\delta_{jn,0} - 1)$ and $\mathbf{P}_n^g$ of components $[\mathbf{P}_n^g]_J = j_n$, for each set J of conformational indices. Note that these vectors are no longer eigenvectors of the $\mathbf{W}$ matrix for the multivariable problem, because the segmental rotations are not independent due to the configurational-dependent friction, and the coupling introduced by the pentane effect. However, the time integrals of the correlation functions of $\mathbf{P}_n^t$ and $\mathbf{P}_n^g$ can be used, to define effective kinetic rates K_n^t and k_n^g for the conformational transitions. Again, the time integrals are calculated as zero-frequency spectral densities from equation (55), by identifying the array $\mathbf{f}$ with $\mathbf{P}_n^t$ and $\mathbf{P}_n^g$ respectively:

$$k_n = \{\mathbf{P}_n^\dagger \mathbf{S} \mathbf{P}_n - (\mathbf{P}_n^\dagger \mathbf{Q})^2\} / \delta \mathbf{P}_n^\dagger \mathbf{W}^{-1} \mathbf{S}\, \delta \mathbf{P}_n. \tag{66}$$

The relation between the kinetic parameters k_n and the standard kinetic rates for conformational transitions is established by extension to a generic segment of the equalities valid for the $N = 1$ case: $k_1^t = k_g + 2K_t$ and $k_1^g = K_g$.

Some numerical results are briefly discussed in the following. Figures 1 and 2 show a comparison between the effective correlation rates k_n^2 for ^{13}C-H spin-dipole interactions modulated by the internal motions, and the kinetic rate constants k_n^g and k_n^t. In the case of $N = 5$, where all configurations have been included and perfectly tetrahedral angles have been assumed, the magnetic correlation rates appear to be almost the average of the kinetic constants for the elementary $t \rightarrow g$ and $g \rightarrow t$ processes. For the $N = 7$ chain, inclusion of the pentane effect and to a lesser extent the choice of the standard geometry, alter this simple conclusion. It is interesting to note, however, that the kinetic rates follow rather closely the behaviour of the magnetic correlation frequencies, suggesting that kinetic rates, which are much easier to calculate, can be used in many instances to describe at a qualitative level the motional behaviour of experimental quantities.

The definitions of the order parameter S_n and the effective correlation frequencies k_n given above are useful in that they provide molecular interpretations of the model-free parameters necessary to interpret N.M.R. relaxation experiments [37]. The table summarizes some of the results

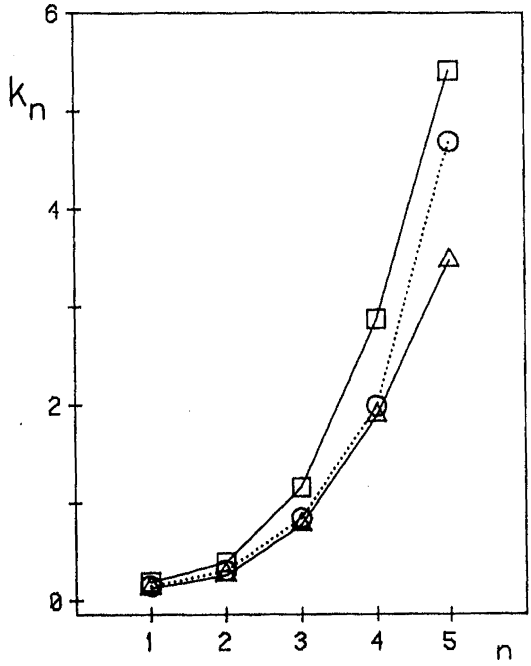

FIGURE 1 Effective rate constants for segmental motions of a $N = 5$ chain, calculated from zero-frequency spectral densities of correlation functions: excess trans population k_n^t (squares), unbalanced gauche population k_n^g (triangles), second-rank tensorial interaction axially symmetric about the C_n-H bond, k_n^2 (circles). The values are in units of w given in equation (40), which can be interpreted as the $g \rightarrow t$ conformational frequency for the $N = 1$ case. All configurations have been included, and regular tetrahedral angles are assumed, with a gauche-trans energy difference $e_g = 0.84$ without pentane effect, and a curvature ratio $\rho = 1$.

calculated for the $N=5$ chain. Two effects are immediately evident: the small, but significant corrections introduced by the inclusion of the pentane effect, and the rapid decrease along the chain of the order parameter, when the value $e_g = 0.84$ is adopted for a standard gauche-trans energy difference of 2.1 kJ and $T = 300$ K, normally suggested for alkyl chains [1]. This means that the conformational motions are able to perform an almost isotropic average of the orientations of the C_n-H bond vectors, except obviously for $n = 1$. In order to obtain higher order parameters in isotropic media, one has to increase the rigidity of the chain by increasing the energy of the gauche configurations. A anomalously large value $e_g = 2.2$ is required to account for the high orientational order parameters experimentally determined by N.M.R. in liquid crystals, if a potential of mean torque

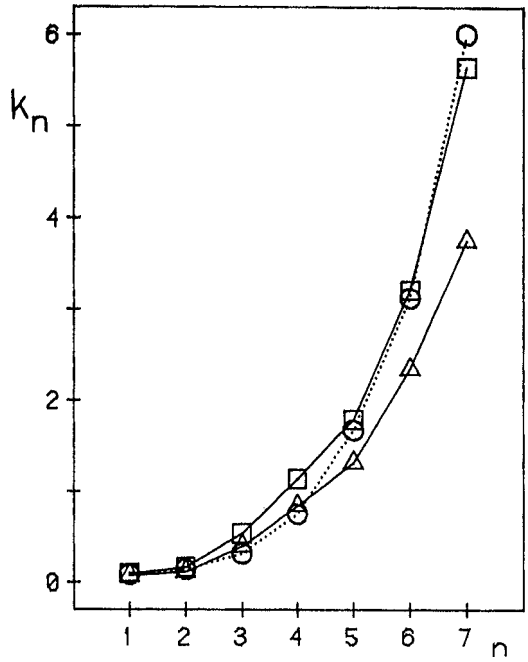

FIGURE 2 Effective rate constants for segmental motions of a $N = 7$ chain, calculated from zero-frequency spectral densities of different correlation functions as in Figure 1. The bond angles $\delta_c = 112°$ and $\widehat{HCH} = 109°$ have been assumed, the number of retained conformers is $N_c = 953$, and pentane effect is included with $e_p = 3$. The values for e_g and ρ are as is Figure 1.

aligning the chain segments along a local director [38] were not explicitly considered.

The variations with respect to the terminal methylene group of the N.M.R. T_1 relaxation times measured at different carbon positions are shown in Figures 3 and 4. They display the zero-frequency spectral densities for second rank correlation functions, including isotropic diffusion of

Effective correlation frequencies in units of w and order parameters for second-rank interaction calculated for $N = 5$ chains with different energy parameters and $\rho = 1$

e_g	e_p	k_1 (S_1)	k_2 (S_2)	k_3 (S_3)	k_4 (S_4)	k_5 (S_5)
0.84	0	0.144 (0.44)	0.301 (0.14)	0.840 (0.10)	2.00 (0.03)	4.60 (0.03)
0.84	3	0.143 (0.50)	0.252 (0.17)	0.589 (0.11)	1.47 (0.04)	3.94 (0.05)
2.20	0	0.099 (0.76)	0.157 (0.57)	0.279 (0.44)	0.493 (0.34)	0.806 (0.27)

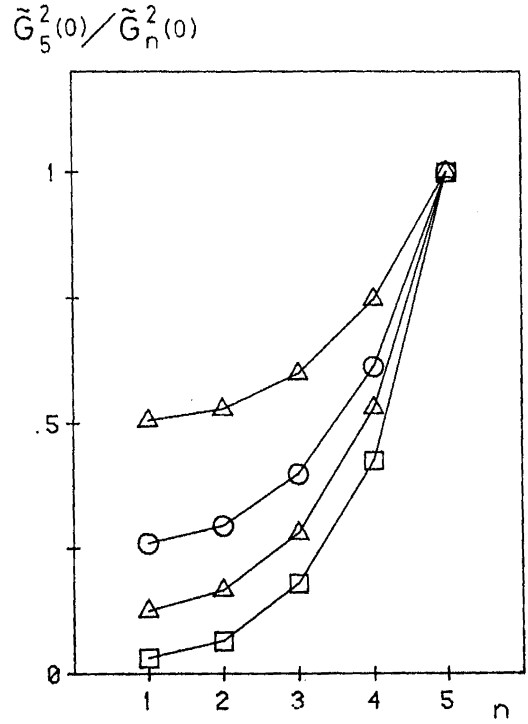

FIGURE 3 Effect of the overall diffusion on C-13 N.M.R. relaxation times, normalized to the value for the last methylene group, in a perfectly regular $N = 5$ chain with $e_g = 0.84$, $e_p = 0$, and increasing ratios D/w: 0.1 (triangles), 0.3 (circles) and 1 (triangles). All configurations are included, and $\rho = 1$. For the sake of comparison, the contribution of the purely conformational motions, calculated from the second term of equation (62) with $D = 0$, is also shown (squares).

the whole molecule, calculated from equation (62) as $\tilde{G}_5^2(0)/\tilde{G}_n^2(0)$. These results are relevant for the interpretation of N.M.R. data under motional conditions of extreme narrowing. These figures differ for the gauche-trans energy difference assumed in the calculations, 0.84 and 2.2 respectively. The various sets of points correspond to increasing ratios of the diffusion coefficient D relative to the elementary frequency w. For the stiffer chain with $e_g = 2.2$, slower diffusional tumblings, relative to the $e_g = 0.84$ case, are required to buffer the effects of the differences in the segmental motions.

In order to exhibit the full frequency dependence of the spectral densities, Cole-Cole plots have been also computed. The imaginary versus the real part of the spectral densities for first-rank interactions calculated from equation (62) are shown in Figures 5–7. The results of Figure 5 are

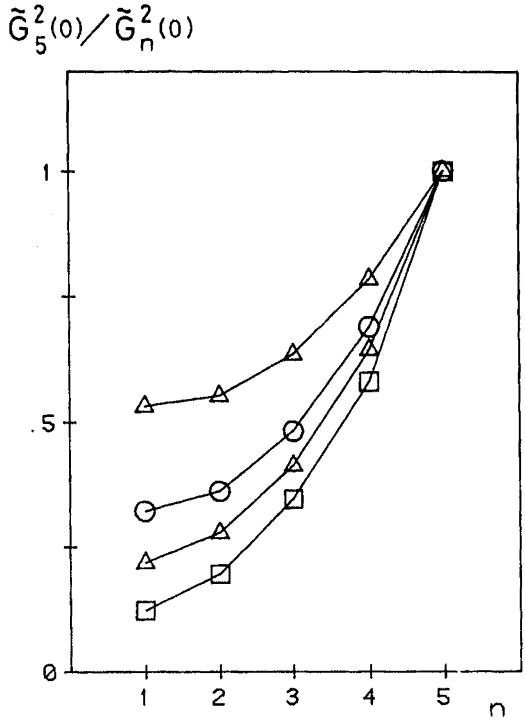

FIGURE 4 Effect of the overall diffusion on the C-13 N.M.R. relaxation times, normalized to the value for the last methylene group in a perfectly regular $N = 5$ chain with $e_g = 2.2$ and increasing ratios D/w: zero (squares), 0.03 (triangles), 0.1 (circles), and 0.4 (triangles). Other parameters as in Figure 3.

calculated under the conditions reported for the Figures 1 and 3 with a diffusion coefficient $D/w = 0.01$; the effect of a larger D value ($D/w = 0.1$) is shown in Figure 6. These results can be easily interpreted by considering that the correlation function for the motion of groups nearest to the core are described by a very large number of exponential decays, whereas the motion of the terminal group is dominated by a single fast decay time, superimposed on the slower contributions coming from the motions of internal segments. These differences are washed out by the overall diffusional motion, when its characteristic frequency approaches the fastest frequency for the internal motions.

The results of the calculations displayed in Figure 7 are obtained with a much higher value for the gauche-trans energy difference, $e_g = 2.2$. In this case the chain is rather rigid, and the spectral densities, even for the most mobile terminal group, have large contributions coming from

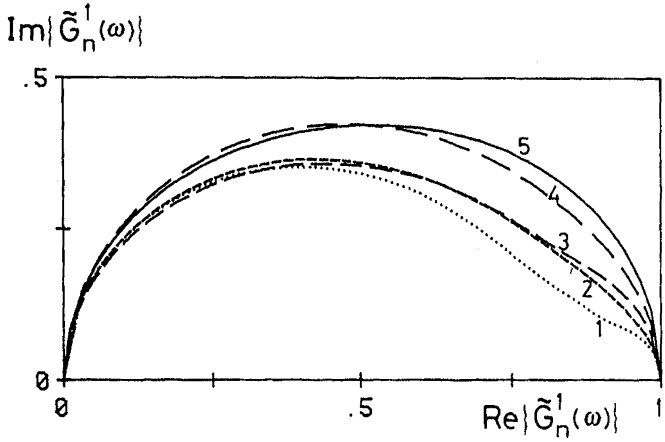

FIGURE 5 Cole–Cole plots for spectral densities relative to motions of a first-rank vectorial property directed along the C_n-H bond, including overall diffusion. $N = 5$ chain with parameters as in Figure 1, and $D/w = 0.01$.

low-frequency motions. In contrast to the previous situation, deviations from a perfect semicircle appear now in the high-frequency side of the Cole–Cole plots. Obviously, in all these cases the correlation function are expressed by complicated superpositions of exponentials, and they can never be described by a single decay time.

In Figure 8, the effect of changing the curvature ratio ρ in the motional rates calculated for $N = 7$ chains is shown. Since an increase of ρ enhances

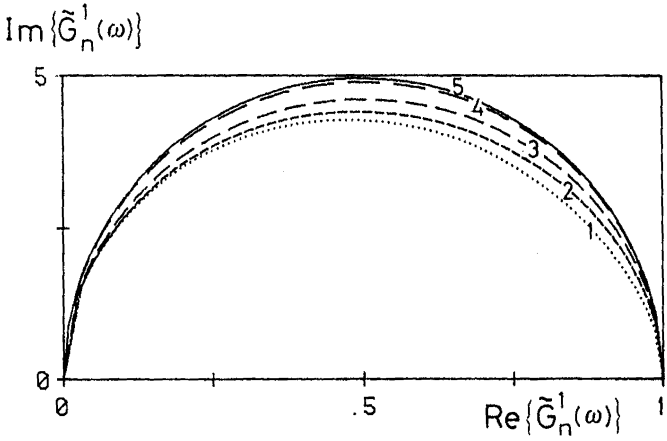

FIGURE 6 Cole–Cole plots as in Figure 4: effect of the increased diffusion coefficient, $D/w = 0.1$.

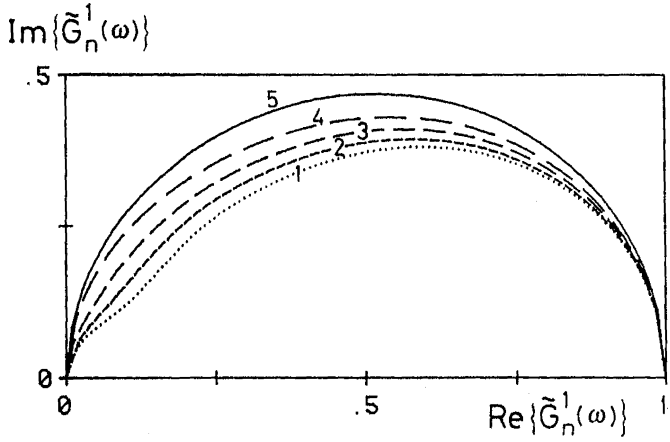

FIGURE 7 Effect on the Cole–Cole profile of the increased rigidity of the $N = 5$ chain due to the increased trans population, for $e_g = 2.2$ and $D/w = 0.03$.

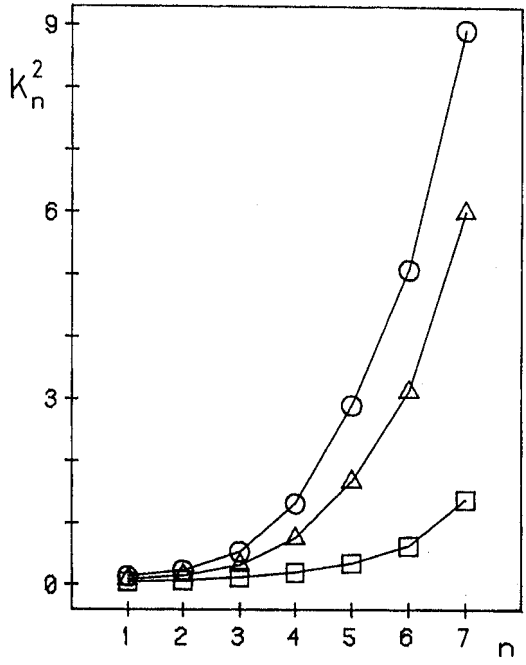

FIGURE 8 Dependence upon the curvature ratio ρ of the effective correlation rates for segmental motions of a $N = 7$ chain, calculated from zero-frequency spectral densities of correlation functions for second-rank tensorial interactions: $\rho = 0$ (squares), 1 (triangles), and 4 (circles). All other conditions are the same as in Figure 2.

cooperation of the torsional motions, we might expect a two-fold effect, i.e. an increase of the relaxation rates due to the fact that transitions are facilitated by distributing the torsions over many segments, and a tendency for them to become independent of the segment position [8].

The transitional rates do actually increase for increasing values of ρ, but the tendency of level off does not show up, probably because our chains are still too short for such an effect to be manifested. Moreover, the model adopted here for the chain, whose fixed end cannot recoil to accompany the conformational transitions of its flexible parts, may introduce an artificial constraint that quenches cooperational motion.

Experimentally, the mobility of the most external ($n = 7$) methylene group in tetra-octylammonium perchlorate, determined by C-13 N.M.R. relaxation, is ten times larger than that observed for the group directly bound to the nitrogen core, when the solvent is methanol [34], and more than 20 times larger in solutions of benzene or dimethyl sulphoxide [39]. The variation of the chain flexibility, going from the constrained end to the free end, has been also revealed very recently by the dramatic changes in the E.S.R. lineshapes of nitroxide spin probes bound to different positions of doxyl stearic acids, attached by the carboxylic function to alumina surfaces [40].

6. CONCLUSIONS

The theoretical model developed here provides a rigorous description of the conformational motions of an alkyl chain, under the assumption that the internal motions can be separated from the overall diffusion of the molecule.

The mathematical derivation differs from others proposed previously in two important respects. First, the matrix for the transitions among the conformational sites is derived by a projection operator procedure, which allows one to obtain an analytical set of localized functions, in the same number of the configurational sites; the discrete master equation is then simply obtained as a matrix representation of the multivariate diffusion operator onto this function subset. Secondly, no factorization of the internal variables has been assumed. The relevant spectroscopic observables are directly computed in terms of spectral densities of suitable correlation functions from the tridiagonal representation of the transition matrix by the Lanczos algorithm. An important ingradient of the model is the definition of configurational vectors, whose correlation functions provide a definition of kinetic rates for specific segmental motions.

Four parameters, all well defined at the microscopic level, enter the calculation: the frequency for the elementary $g \rightarrow t$ conformational transition, the ratio of the curvatures of the potential surface in reactive

and non-reactive modes, the energy difference between gauche and trans conformers, and the repulsive term for hindered sequences. In a simplified version, by using a weighted average of the transition matrix elements in place of time integrals of correlation functions, the model has been shown to interpret correctly the C-13 N.M.R. relaxation in tetra-alkylammonium ion salts [34].

A number of criticisms could obviously arise. As already mentioned, the recoil of the 'head' of the chain to the conformational transitions of the tail has been ignored so far, but there is little doubt that it could be incorporated into the theory. Inclusion of 'hard' modes, such as skeleton bending modes, also appears to be required for an accurate computation of thermodynamic properties [25]. The most crucial point is however the neglect of the 'fast' jiggering motions inside the potential wells. In the case of long tails, large amplitude and low frequency modes might result from the coupling of such motions, invalidating the projection procedure which identifies the conformational jumps as the unique slow process. Even if the chains considered in the present work are short enough to justify the time-scale separation implicit in the projection procedure, it is certainly safe to devise a method of checking the limits of the RIS approximation, when applied to the description of the dynamical behaviour of polymeric chains.

REFERENCES

[1] Flory, P. J. (1969). *Statistical Mechanics of Chain Molecules*. Wiley.
[2] Wallach, D. (1967). *J. chem. Phys.*, *47*, 5258.
[3] Levine, Y. K., Birdsall, N. J. M., Lee, A. G., & Metcalfe, J. C. (1974). *J. chem. Phys.*, *60*, 2890.
[4] London, R. E. & Avitable, J. (1977). *J. Am. Chem. Soc.*, *99*, 7765; (1978) *Ibid.*, *100*, 7159.
[5] Wittebort, R. J. & Szabo, A. (1978). *J. Chem. Phys.*, *69*, 1722; Wittebort, R. J., Szabo, A., & Gurd, F. R. N. (1980). *J. Am. Chem. Soc.*, *102*, 5723.
[6] Edholm, O. & Blomberg, C. (1979). *Chem. Phys.*, *42*, 449.
[7] Kramers, H. A. (1940). *Physica*, *7*, 284.
[8] Skolnick, J. & Helfand, E. (1980). *J. Chem. Phys.*, *72*, 5489.
[9] Helfand, E. & Skolnick, J. (1982). *J. Chem. Phys.*, *77*, 5714.
[10] Langer, J. S. (1969). *Ann. Phys.*, *54*, 258.
[11] Levy, R. M., Karplus, M., & McCammon, J. A. (1979). *Chem. Phys. Lett.*, *65*, 4.
[12] Levy, R. M., Karplus, M., & Wolynes, P. G. (1981). *J. Am. Chem. Soc.*, *103*, 5998.
[13] Happel, J. & Brenner, H. (1965). *Low Reynolds Number Hydrodynamics*. Prentice-Hall.
[14] Moro, G. & Nordio, P. L. (1985). *Molec. Phys.*, *56*, 255.
[15] Moro, G. & Nordio, P. L. (1986). *Molec. Phys.*, *57*, 947.
[16] Moro, G. & Nordio, P. L. (1986). *Z. Phys. B*, *64*, 217.
[17] Borgis, D. & Moreau, M. (1986). *Molec. Phys.*, *57*, 33.
[18] Chandler, D. (1978). *J. Chem. Phys.*, *68*, 2959; Montgomery, J. A., Chandler, D. & Berne, B. J. (1979). *J. Chem. Phys.*, *70*, 4056.
[19] Skinner, J. L. & Wolynes, P. G. (1978). *J. Chem. Phys.*, *69*, 2143; (1980) *Ibid.*, *72*, 4913.

[20] Garrity, D. K. & Skinner, J. L. (1983). *Chem. Phys. Lett.*, *95*, 46.
[21] Schuss, Z. (1980). *Theory and Applications of Stochastic Differential Equations*. Wiley.
[22] Van Kampen, N. G. (1981). *Stochastic Processes in Physics and Chemistry*. North-Holland.
[23] Szabo, A., Schulten, K., & Schulten, Z. (1980). *J. Chem. Phys.*, *72*, 4350.
[24] Hänggi, P. (1986). *J. Statist. Phys.*, *42*, 105.
[25] Karplus, M. & Kushick, J. N. (1981). *Macromolecules*, *14*, 325.
[26] Rose, M. E. (1957). *Elementary Theory of Angular Momentum*. Wiley.
[27] Scott, R. A. & Scheraga, H. A. (1966). *J. Chem. Phys.*, *44*, 3054.
[28] Ryckaert, J. P. & Bellemans, A. (1975). *Chem. Phys. Lett.*, *30*, 123.
[29] Chachaty, C. & Langlet, G. (1985). *J. Chem. Phys.*, *82*, 613.
[30] EISPACK, Argonne Code Center, Argonne National Laboratory.
[31] Moro, G. & Freed, J. H. (1981). *J. Chem. Phys.*, *74*, 3757.
[32] Moro, G. & Freed, J. H. (1986). In: *Large Scale Eigenvalue Problems*, Cullum, J. K. & Willoughby, R. A. (eds.). North-Holland.
[33] Cullum, J. K. & Willoughby, R. A. (1985). *Lanczos-Algorithms for Large Symmetric Eigenvalue Computations*, Birkhauser, Vol. I.
[34] Coletta, F., Moro, G., & Nordio, P. L. (1987). *Molec. Phys.*, *61*, 1259.
[35] Meier, P., Ohmes, E., & Kothe, G. (1986). *J. chem. Phys.*, *85*, 3598.
[36] Evans, G. T. (1983). In: *Molecular-Based Study of Fluids*, Haile, J. M. & Mansoori, G. A. (eds.). American Chemical Society.
[37] Lipari, G. & Szabo, A. (1982). *J. Am. Chem. Soc.*, *104*, 4546; *Ibid.*, *104*, 4559.
[38] Emsley, J. W., Luckhurst, G. R., & Stockley, C. P. (1982). *Proc. R. Soc. A*, *381*, 117.
[39] Coletta, F., Ferrarini, A., & Nordio, P. L. (to be published).
[40] Chandar, P., Somasundaran, P., Waterman, K. C., & Turro, N. J. (1987). *J. Phys. Chem.*, *91*, 148.